



# Three-Dimensional Finite Element Based Numerical Simulation of Machining of Thin-Wall Components with Varying Wall Constraints

Shrikrishna Nandkishor Joshi<sup>1</sup> · Gururaj Bolar<sup>1</sup>

Received: 20 March 2015 / Accepted: 11 May 2016 / Published online: 14 June 2016  
© The Institution of Engineers (India) 2016

**Abstract** Control of part deflection and deformation during machining of low rigidity thin-wall components is an important aspect in the manufacture of desired quality products. This paper presents a comparative study on the effect of geometry constraints on the product quality during machining of thin-wall components made of an aerospace alloy aluminum 2024-T351. Three-dimensional nonlinear finite element (FE) based simulations of machining of thin-wall parts were carried out by considering three variations in the wall constraint viz. free wall, wall constrained at one end, and wall with constraints at both the ends. Lagrangian formulation based transient FE model has been developed to simulate the interaction between the workpiece and helical milling cutter. Johnson–Cook material and damage model were adopted to account for material behavior during machining process; damage initiation and chip separation. A modified Coulomb friction model was employed to define the contact between the cutting tool and the workpiece. The numerical model was validated with experimental results and found to be in good agreement. Based on the simulation results it was noted that deflection and deformation were maximum in the thin-wall constrained at one end in comparison with those obtained in other cases. It was noted that three dimensional finite element simulations help in a better way to predict the product quality during precision manufacturing of thin-wall components.

**Keywords** Thin-wall machining · End milling · Numerical simulation · Deformation · Deflection · Aluminum 2024-T351 · Finite element method

## Introduction and Literature Review

To reduce the weight of an aircraft, design and development of monolithic structural components containing thin webs and ribs have become inevitable nowadays. Manufacturing of these components using machining operation has low productivity because approximately 90–95 % of the material from the initial work material volume gets removed during the operation [1]. Moreover, the thin-wall structures possess low stiffness and often deflect and deform under the action of cutting forces. In-process deflection and deformation of work-parts lead to geometrical errors which influence the accuracy and quality of the machined part. Researchers proposed that the machining errors can be minimized either by trial and error approach or by repetitive feeding techniques. However, this may result in higher lead time and production cost.

Literature reports experimental studies on various aspects of thin-wall machining which include effects of various parameters like cutting tool geometry [2–4], cutting forces [5], thin-wall deflection [6], machining stability and chatter [7, 8] error prediction and control [9, 10], part deformation [11] and machining temperature [12]. Jabbaripour et al. [2] studied the influence tool path strategies on surface texture of machined thin-wall part. Izamshah et al. [3] studied the effect of variation in end mill helix angle on accuracy during machining of thin-rib aerospace components. It was observed that larger helix angle produced minimum chatter resulting in least surface error compared to a smaller diameter tool. Jiang et al. [4] studied

✉ Shrikrishna Nandkishor Joshi  
snj@iitg.ac.in

<sup>1</sup> Indian Institute of Technology Guwahati, Guwahati 781 039, Assam, India

the effects of tool diameter on the residual stress and distortion induced by milling of thin-walled part. Authors concluded that larger diameter tool reduces the distortion and residual stresses in thin-wall workpiece. A study on the effect of input process parameters on cutting forces and deformation during the machining process was reported by Tanase et al. [5]. Cao et al. [6] worked on deformation analysis of thin-wall components made of aluminum alloy. However, it has been noted that most of these work were restricted to study on free wall components. Industrial thin walled components have thin ribs which may be constrained by other walls at their ends. In-process deflection and deformation during machining of such walls with different constraints may vary as compared with those obtained for free wall structure. Very scant work has been reported on the effect of variation in geometrical constraints on product quality of thin-walls parts.

Literature also depicts numerical and analytical studies on machining of thin-wall components. Seguy et al. [7] studied the link between chatter instability and surface roughness evolution for thin wall milling by using stability lobe theory to develop a numerical model. Campa et al. [8] analyzed the problem of the variable dynamics in thin-wall machining and solved it through the calculation of 3D stability lobes where a third dimension with the tool position is added along with the traditional depth of cut-spindle speed pair. Chen et al. [9] predicted the deformation during multilayer machining of thin-wall parts using single tooth cutter and further compensated the work surface errors. Ratchev et al. [10] developed an integrated methodology for modeling and prediction of surface errors caused due to deflection of the thin-wall components. They developed a cutting force and material removal model algorithm and combined them with part model data. This integrated model was used for simulating the part behavior during thin-wall machining thus helping in determining the part deflection. Ning et al. [11] suggested two approaches to solve the problem of deformation in thin-wall milling. The first one was to reduce the deformation by using high speed machining, and the second one was by over-cutting the wall to remove the remaining material by numerically controlled (NC) compensation. Rai and Xirouchakis [12] analyzed the errors induced during milling of thin-wall components by carrying out experimental and numerical work to measure the cutting force components, work piece temperature distribution, part deflection, and stresses during the process. Ratchev et al. [13, 14] reported to have developed a flexible cutting force model and utilized it to predict the deflection of thin-wall part. Aijun and Zhan-qiang [15] studied static deformations of thin-walled plate under the action of end milling forces by developing an analytical model. The deformation was predicted with the help of theoretical deformation equations based on the

reciprocal theorem. The influences of cutter location, linear loads and thickness of plates on deformation of flexible part were taken into consideration. However, it has been noted that in most of the cases the cutting forces were obtained either experimentally or by analytical force modeling which provided input to determine the deflection and deformation of the straight walled part. Also the cutting force and deflection values were computed based on certain assumptions viz. simplification of milling force as linear load [15], equating the component to a thin-plate and utilizing thin plate theory to analyze the deflection [16]. Some researchers assumed that material of the workpiece deformed in a stable elastic manner in thin-wall machining process [11]. These assumptions limit the applications of above-mentioned models. A need was thus identified to carry out three-dimensional nonlinear numerical simulation of physical interaction between helical milling cutter and workpiece to study the effect of wall constraints on the quality of the thin-wall product.

### Finite Element Simulation of Thin-Wall Machining Process

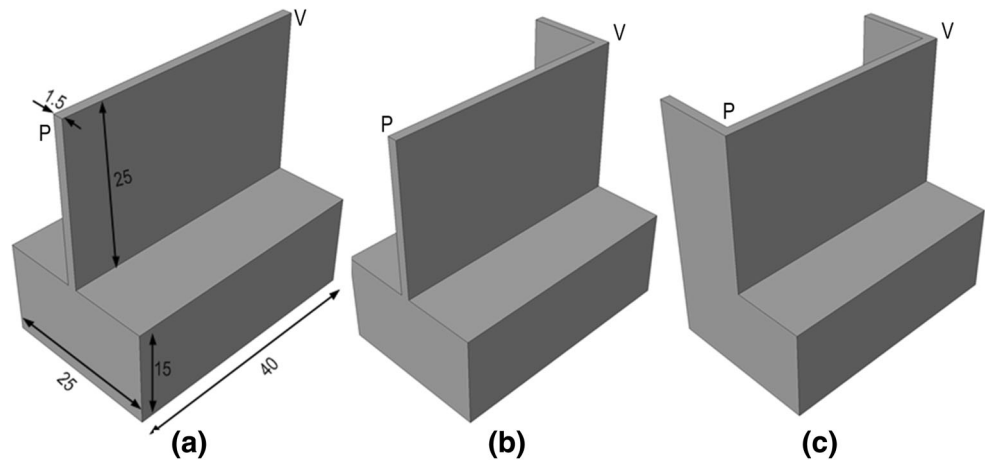
Though the two-dimensional modeling is computationally inexpensive and efficient, it does not simulate the cutting interaction between the helical teeth of milling cutter and the workpiece. Thus it has limited applicability. Moreover, in two-dimensional simulation, it is difficult to predict the workpiece deformation and deflection due to constraints at the workpiece boundaries. Therefore, it was felt worth to develop a three-dimensional finite element model that would provide a more realistic simulation of thin-wall machining operation.

In this work, three dimensional nonlinear finite element based numerical simulations have been carried out to study the effect of geometry constraints on the deformation and deflection of thin walled parts. Three cases viz. free wall, wall constrained at one end and wall constrained at both the ends were chosen for the analysis. The simulation model was developed by using the material constitutive criterion for describing the material behavior of aluminum 2024-T351 alloy with material damage law for chip separation. The details of model development are reported subsequently.

### Geometrical Modeling, Boundary Conditions and Mesh Configuration

In the present work, commercial FEM solver ABAQUS<sup>TM</sup> was used to simulate the cutting process. In practice, the thin-wall components may have free ends (without any constraints) or in some cases the main wall may be

**Fig. 1** Different geometries of workpiece: **a** free wall, **b** wall constrained at one end, and **c** wall constrained at both ends



constrained by side walls at one or both ends. In the present work three workpiece models with various shapes as shown in Fig. 1 are considered for the comparative performance study.

For case (a), the workpiece was constrained at the bottom, whilst the other three ends of the thin-walled part were not constrained with any boundary conditions as shown in Fig. 2. The milling tool was provided with a linear motion in the feed direction and is also provided with rotation motion about its axis. However, for case (b) the wall was also constrained at end V, whilst for case (c), both the ends P, V were constrained.

The workpiece was meshed with 3D solid element C3D8R. This element is of 8-node linear brick type with reduced integration and hourglass control. To reduce the computation and analysis time, the cutting region where tool and workpiece interaction takes place was only fine meshed, other part of the work was coarse meshed. It helped in capturing the chip formation process at the cutting region and minimized the use of total numbers of elements for the computation. The workpiece was discretized into 293,745 elements. The cutting tool was considered to be a rigid body and was discretized into 12,650 elements. Cutting tool parameters related to the end mill are listed in Table 1.

**Material Properties and Material Constitutive Equation**

Aluminum alloy 2024-T351 (A2024-T351), an aerospace material, was used in this work. The constitutive material model proposed by Johnson–Cook (J–C) was adopted which takes care of effect of various material parameters viz. plastic strain, strain rate, process temperature on the flow stress of the material [18]. As per J–C model the equivalent plastic flow stress is given as,

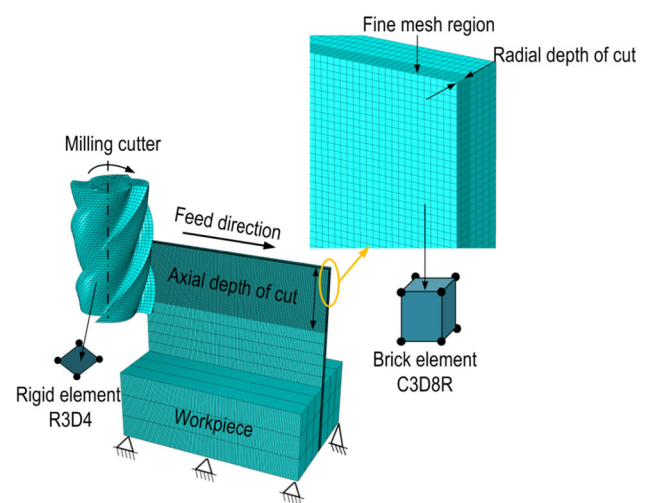


**Fig. 2** Boundary conditions and part meshing for a free-wall structure

**Table 1** Cutting tool parameters [17]

Tool material	HSS
Tool diameter (mm)	08
Tool rake angle (°)	12
Tool helix angle (°)	30
Tool clearance angle (°)	15
Number of flutes	04

$$\bar{\sigma} = (A + B\epsilon^n) \left[ 1 - C \ln \left( \frac{\dot{\epsilon}}{\dot{\epsilon}_0} \right) \right] \left( 1 - \left( \frac{T - T_{room}}{T_{melt} - T_{room}} \right)^m \right) \tag{1}$$

where, *A* (MPa) is the initial yield stress of the material, *B* (MPa) the hardening modulus, *C* the strain rate dependency coefficient, *n* the work-hardening exponent, *m* the thermal softening coefficient,  $\epsilon$  is the equivalent plastic strain,  $\dot{\epsilon}$  is the equivalent plastic strain rate and  $\dot{\epsilon}_0$  is

**Table 2** Johnson–Cook material parameter values for A2024-T351 [19]

A	B	n	C	m
352	440	0.42	0.0083	1

**Table 3** Johnson–Cook failure parameters for A2024-T351 [19]

$D_1$	$D_2$	$D_3$	$D_4$	$D_5$
0.13	0.13	−1.5	0.011	0

**Table 4** Workpiece material properties [19]

Density, $\rho$ (kg/m <sup>3</sup> )	2700
Elastic modulus, $E$ (GPa)	73
Poisson ratio, $\nu$	0.33
Specific heat, $C_p$ (J/kg °C)	$=0.557 T + 877.6$
Thermal expansion, $\alpha$ (10e − 6/ °C)	$=8.9 \times 10^{-3} T + 22.2$
Thermal conductivity, $\lambda$ (W/m °C)	$25 \leq T \leq 300$ $=0.247 T + 114.4$ $300 \leq T \leq T_{melt}$ $=-0.125 T + 226$
Melt temperature, $T_{melt}$ (°C)	520
Room temperature, $T_{room}$ (°C)	25

**Table 5** Cutting condition during machining

Cutting condition	Dry
Spindle speed, $n$ (rev/min)	6000
Feed, $f_t$ (mm/tooth)	0.15
Radial depth of cut, $d_r$ (mm)	0.3
Axial depth of cut, $d_a$ (mm)	12.5

reference plastic strain rate,  $T_{room}$  is the room temperature and  $T_{melt}$  is the workpiece melting temperature. The Johnson–Cook parameter values for aluminum A2024-T351 are listed in Table 2.

**Material Failure and Chip Formation**

Material failure refers to the complete loss of load carrying capacity which results from progressive degradation of the material stiffness. Progressive damage and failure can be modeled in materials using Johnson–Cook failure model [20]. Lagrangian model with element deletion algorithm was employed for the simulation of complex three dimensional machining process. This model uses damage

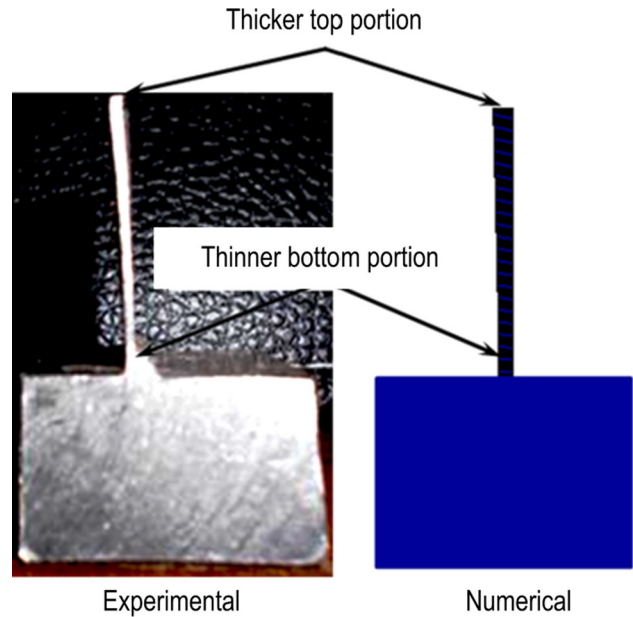


**Fig. 3** Comparison of form error obtained during experiments [22] and our numerical simulation

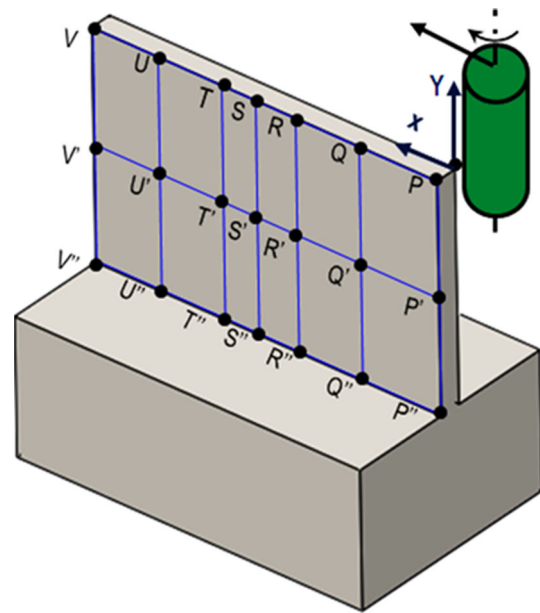


**Fig. 4** Deflection data measurement points for free-wall structure

parameter  $D$  which is defined as the sum of the ratio of the increments in the equivalent plastic strain  $\epsilon$  to the fracture strain  $\epsilon_f$ . The expression of  $D$  is given as,

$$D = \sum \frac{\Delta\epsilon}{\epsilon_f} \tag{2}$$

The equivalent fracture strain  $\epsilon_f$  was determined by using the equation

$$\varepsilon_f = \left[ D_1 + D_2 \exp\left(D_3 \frac{P}{\bar{\sigma}}\right) \right] \left[ 1 + D_4 \ln\left(\frac{\dot{\varepsilon}}{\dot{\varepsilon}_0}\right) \right] \left( 1 + D_5 \left(\frac{T - T_{room}}{T_{melt} - T_{room}}\right) \right) \tag{3}$$

where  $D_1$  to  $D_5$  are the damage constants,  $P$  is the hydrostatic pressure and  $\bar{\sigma}$  is equivalent flow stress. Constants of J–C failure model for A2024-T351 are tabulated in Table 3. As per J–C damage law, when the damage parameter  $D$  equals unity the material loses its load carrying capacity and failure occurs. Thus the elements showing the value of  $D$  equal to 1 were chosen and then deleted. The workpiece material properties are listed in Table 4.

### Workpiece and Cutting Tool Contact

The friction condition at the tool and workpiece interface influences the cutting forces, temperature, machining quality and tool wear. The contact between the cutting tool and the workpiece was defined by using modified

Coulomb friction model. As per this model the contact between the chip and the rake surface region can be divided into two regions viz. the sliding region and the sticking region [21]. Sticking friction occurs very near to the cutting edge in contact with the workpiece and the sliding friction occurs far away from the contact area. The sliding region obeys the Coulomb friction law. In the sticking region, the shear stress  $\tau$  is equal to the critical frictional stress. The modified Coulomb law is defined by following equations,

$$\tau = k_{chip} \quad \text{when } \mu\sigma > k_{chip} \quad (\text{Sticking region}) \tag{4}$$

$$\tau = \mu\sigma \quad \text{when } \mu\sigma < k_{chip} \quad (\text{Sliding region}) \tag{5}$$

where  $\tau$  is the frictional stress,  $\sigma$  is the normal stress and  $k_{chip}$  is the shear flow stress of material. The co-efficient of friction  $\mu$  was considered as 0.17 [19]. Advantage of using the modified Coulomb friction model is that the solver determines the friction state automatically according to the contact stress value during the simulation process.

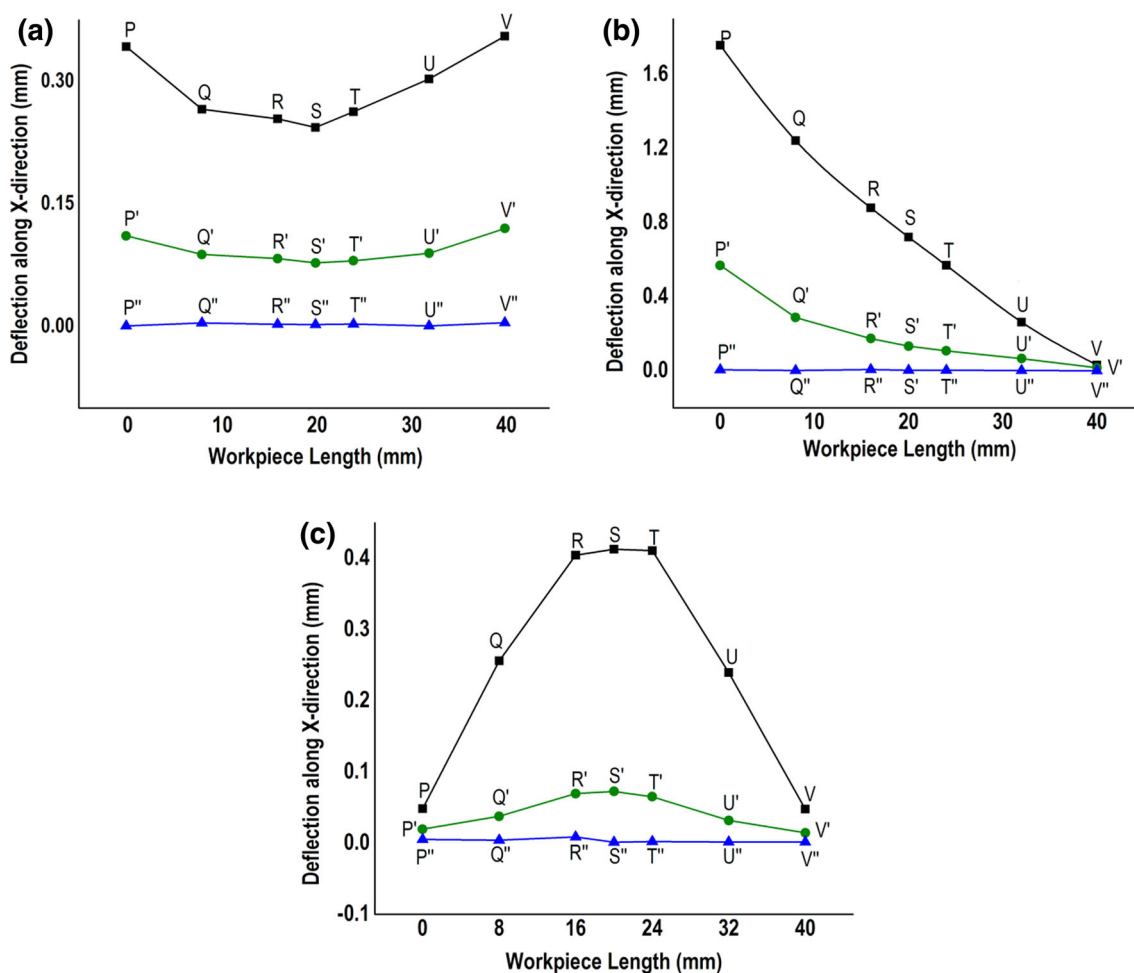


Fig. 5 Maximum deflection along the along the length of workpiece

## Cutting Conditions and Process Simulation

In this work, Lagrangian formulation based 3D finite element simulation of thin-wall machining has been carried out using an end milling cutter. The cutting conditions are listed in the Table 5. Heat generated due to friction and plastic deformation during machining were neglected to reduce the computation time and to help in the better memory management. ABAQUS<sup>TM</sup> explicit software was used to carry out the simulation work. Total simulation time taken in each case was about 52 h with 3.4 GHz, 4 GB RAM processor.

## Experimental Validation of Numerical Simulations

Experimental studies on constraint free thin-wall part made of aluminum alloy were carried out by Mangalekar [22] on a 3-axis CNC milling machine with FANUC controller. Experiments were planned and carried out by varying the process parameters viz. spindle speed, feed rate, axial and

radial depth of cut. The deflection data was collected during the process using a linear variable differential transformer (LVDT) sensor. Based on the work carried out, average deflection at the top edge was observed to be 0.362 mm. In the present 3D numerical simulations, an average deflection of about 0.289 mm was obtained at the top edge. The proposed model predicted a lesser value of deflection in comparison with that obtained by Mangalekar [22]. However, it was found in quite good agreement. The error in prediction may be due to the fact that the proposed model does not consider the errors generated due to machine tool inaccuracies, vibrations and chatter, work-piece and tool setting, thermal expansion of workpiece etc.

Figure 3 shows a comparison of the side view of machined workpiece obtained during the experimental work [22] and the present numerical work. In both the cases it was observed that the deflection at the top edge was more as compared to the bottom portion of the workpiece. This may be due the fact that the inverted cantilever is just fixed at its bottom portion whilst its top portion is free and unconstrained which deflect under the action of resultant

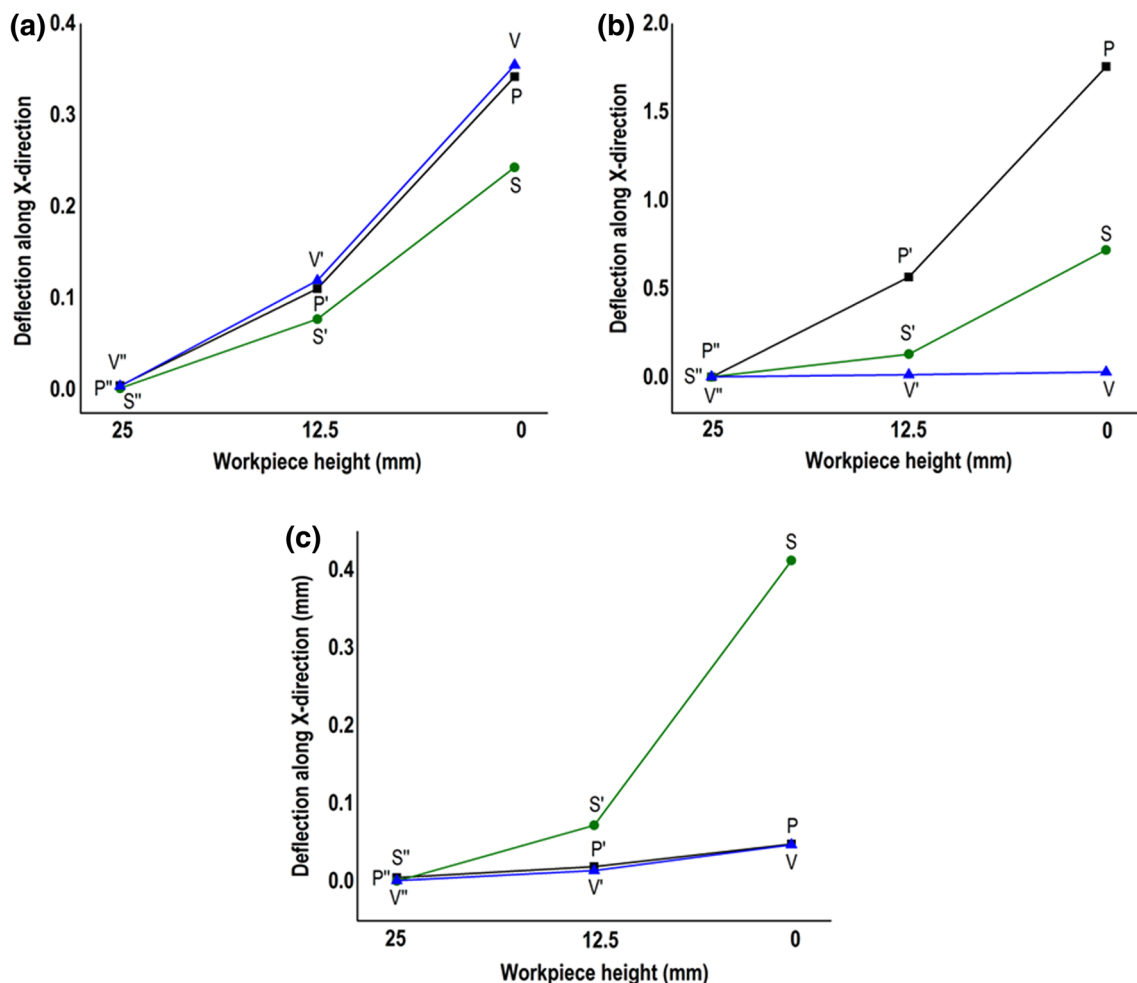


Fig. 6 Maximum deflection along the along the height of workpiece

force. As a result material remains uncut at the top end. Also it is observed that the thin-wall structure had undergone permanent deformation in both the type of studies. Thus numerical simulation reported here verifies the established facts which are observed during experimental studies [22]. This provided a confidence to carry out the numerical simulations to predict the deflection and deformation by varying the wall geometry constraints by using the developed model. However, more systematic experiments with sophisticated instruments are in process to validate the results in terms of forces predicted by our numerical simulations.

### Results and Discussion

In this work the effect of wall geometry constraint on the in-process deflection and permanent deformation of thin-wall structure has been studied. For this purpose, the deflection data were recorded at various points over the free wall as per

a scheme shown in Fig. 4. Similar schemes were employed for the other two cases. The cutter was allowed to move along X-direction from point ‘P’ to ‘V’. Deflection data along X-direction after completion of each cut pass were recorded for all three cases and plotted as shown in Fig. 5.

Figure 5a shows the variation of in-process deflection along workpiece length for a free-end thin wall. In this case it is observed that the maximum deflection occurs at the two ends compared to the center of the thin-wall. This may be due the fact that the two ends of the workpiece are free ends which are flexible hence deflect under the action of resultant cutting forces. However, in case of the wall constrained by a side wall at one end (see Fig. 5b), deflection was found to be maximum at the free end as compared with that occurred at the fixed end. It is because the free end being less rigid, easily deflect under the action of cutting forces. In case of wall constrained on both the ends, the deflection was found to be more at the center (see Fig. 5c). Also it can be observed that the wall constrained at one end has undergone maximum deflection as

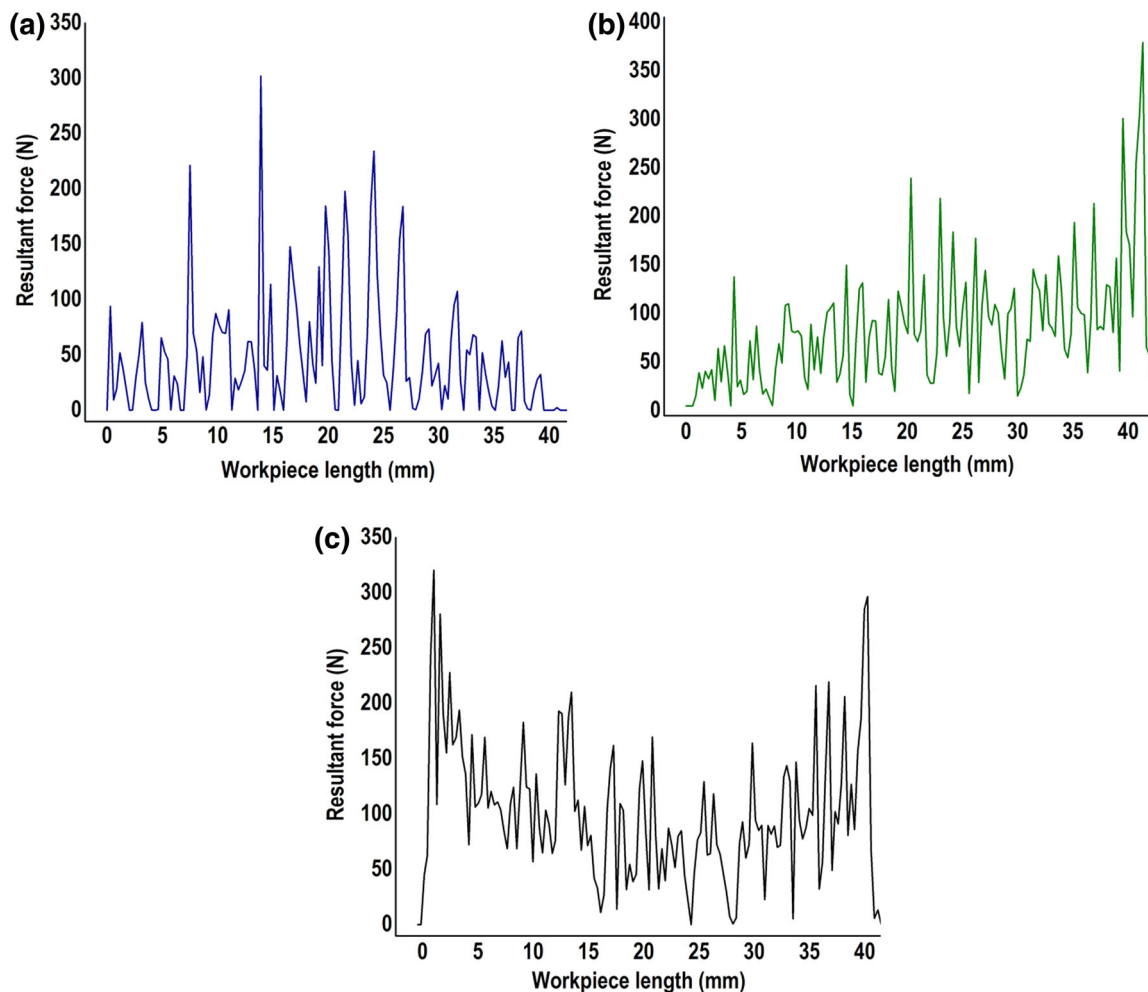


Fig. 7 Resultant cutting force during machining of thin-walls: a free wall, b wall constrained at one end, and c wall constrained at both ends

compared to the other cases. It may be due to fact that the cutting forces pushes and holds the wall in its deflected position during the entire period of contact of milling cutter with the work material. Thus it produces the maximum deflection as compared with that obtained in other cases.

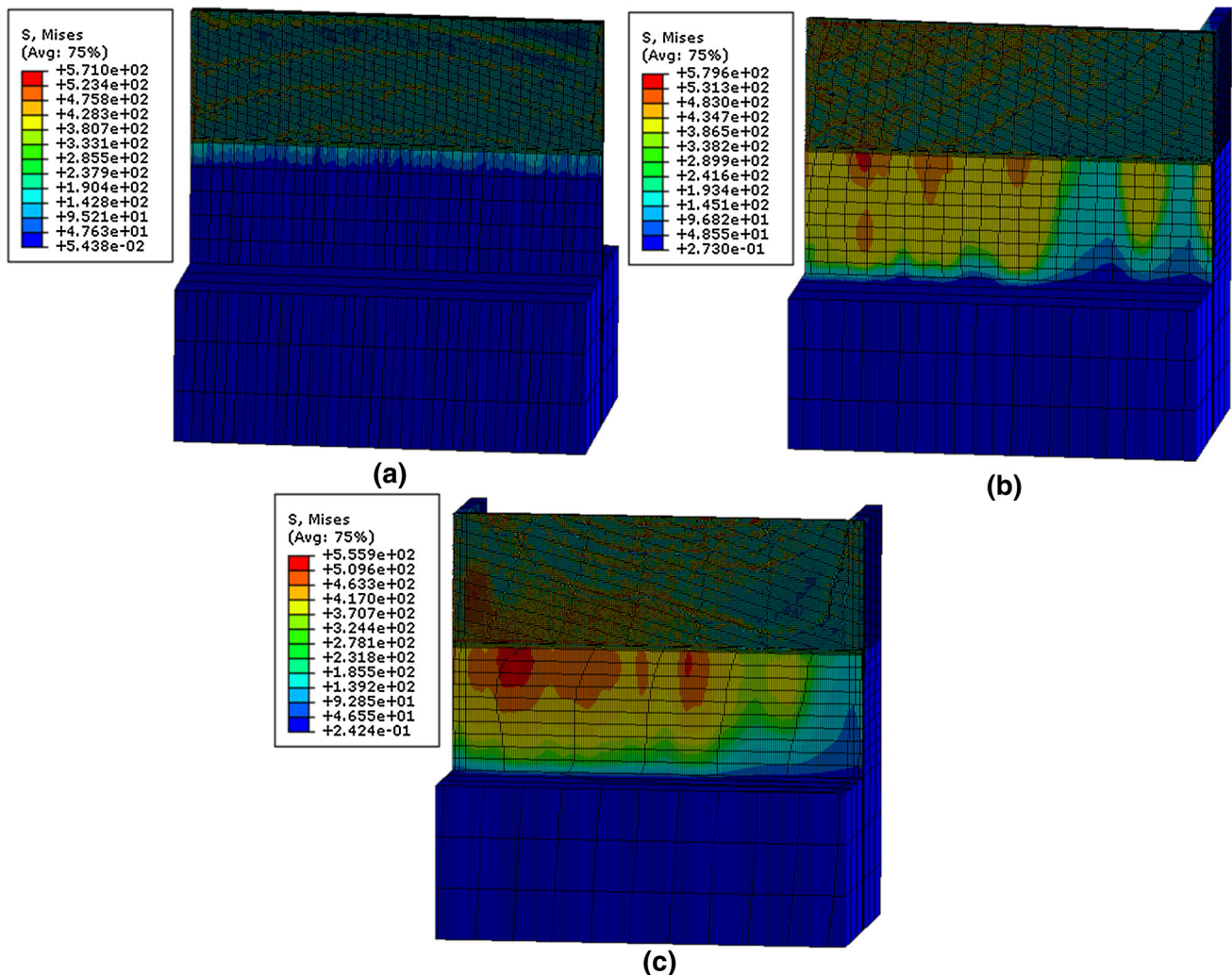
Figure 6 shows the variation of deflection along the height of the workpiece during the milling operation. It can be observed that in all three cases, the maximum deflection occurs at the top edge of the thin-wall as compared to that of the wall base. The top edge of the thin-wall part is free and unconstrained, and is less rigid. Hence, it deflects more as compared to the base which is supported with the surrounding bulk material.

Figure 7a shows the resultant cutting force data during milling of constrain free wall. It can be observed that resultant cutting force was lower at the tool entry end, attains the maxima as the tool reached in the middle and then gradually reduced as the tool exits after the machining. This is because of the fact that due to low rigidity at the ends

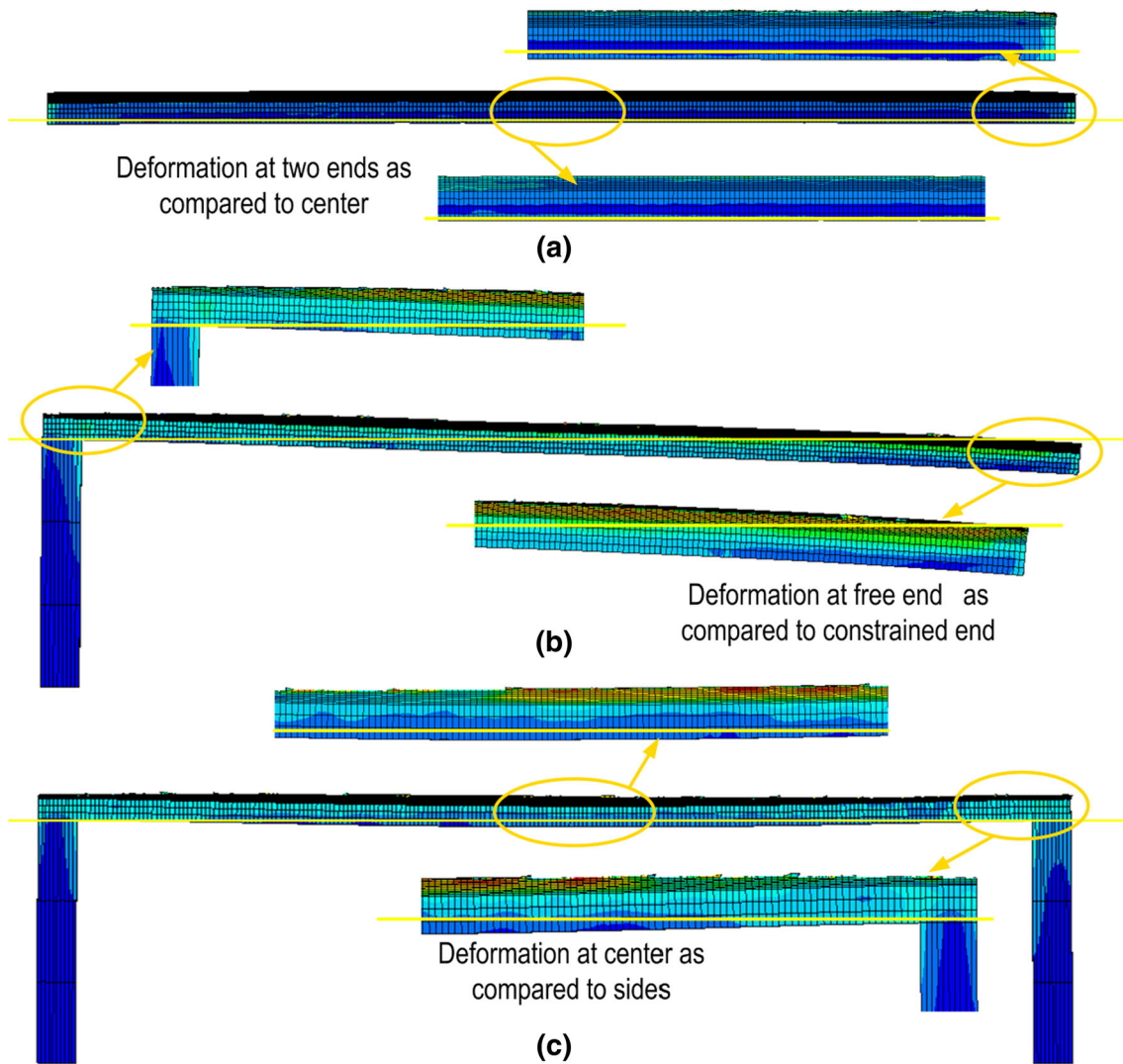
of the part, the deflection is more and thus the part resist less to the plastic deformation. However, in comparison with the ends, the rigidity at the middle is high and hence the cutting forces are of higher values. For the wall constrained at one end the resultant force was lower at the low rigidity free end and gradually increased as the tool reached constrained end (see Fig. 7b). From Fig. 7c it can be observed that, in the case of wall constrained at both ends the resultant force was higher at two ends in comparison with that at the middle of the wall. The two ends are rigid constrained ends as compared to the middle of the wall which is free to deflect under the action of resulting forces.

Figure 8 shows the stress distribution at the end of milling operation in all the three cases. It should be noted that in all the three cases maximum stresses are higher than the materials yield strengths of around 372 MPa [23]. As a result the walls show signs of deformation in plastic domain.

Figure 9 shows the top section of the walls after the machining operation. It was noted that during thin-wall



**Fig. 8** Stress distribution in machined thin-walls: **a** free wall, **b** wall constrained at one end, and **c** wall constrained at both ends



**Fig. 9** Top section view of parts with indication of permanent deformation

machining some portions of the wall remain thicker. It may be due to the in-process deflection and deformation of the walls during the cutting operation. It is noted that some amount of permanent deformation occurs in all the three cases. In case of a free wall (see Fig. 9a), it can be observed that the free wall has undergone some amount of permanent deformation at the two low rigidity ends as compared to that obtained at the center. The thin-wall constrained at one end shows permanent deformation at its free end. Also the amount of deformation (Fig. 9b) is substantially higher as compared that recorded in the other two cases. As discussed earlier, in case of a thin-wall constrained at one end the cutting forces push and hold the wall in its deflected position during the entire period of contact of milling cutter with the work material. The workpiece is stressed beyond its material yield stress value leading to permanent deformation in the thin-wall. In the third case, it is observed that there is no permanent

deformation at the ends as it was constrained. However, at the center, the wall was stressed beyond the material yield value and the wall had undergone deflection leading to some amount of permanent deformation (Fig. 9c). The amount of deflection was comparatively less in comparison with that obtained for the wall constrained at one end. Thus three-dimensional simulations help to predict the product quality in terms of deflections and sections thickening during the thin-wall machining operations. These predictions provide guidelines and process conditions for obtaining the desired product quality.

## Conclusions

In the present work, three dimensional nonlinear finite element based numerical simulation of thin-wall machining of various wall constrain configurations were carried out.

In comparison with the 2D simulations, this 3D simulation provided more realistic picture of the physical interaction of workpiece and helical milling cutter in terms of study of important process parameters such as in process deflection and permanent deformation. The approach was found to be realistic as it employs the Johnson–Cook material model and damage law to define the workpiece material properties and chip formation criterion along with a contact model. A significant amount of in-process deflection was observed in all three cases of thin-wall geometries. In the case of thin wall with only one end constrain, the maximum deflection was noticed with that obtained in other cases. The thin walls were found to be deformed permanently under the action of cutting forces. The deformation and deflection were found to be affecting the section thickness of the cut walls. In the case of wall constrained at one end, the thickening of cut wall was noted to be more in comparison with that obtained in other cases. It was thus affecting the quality of the machined wall in terms of uniform cross section of wall. It is noted that proper selection of cutting parameters like cutting speed, feed rate, and depth of cut is necessary to control the deflection and deformation of the thin-wall parts to improve the product quality. A work in this direction is under progress.

**Acknowledgements** This article is a revised and expanded version of the paper entitled “3D finite element modeling of thin-wall machining of aluminum 7075-T6 alloy” presented at AIMTDR 2014 organized by Indian Institute of Technology Guwahati, Guwahati, India during 12–14 December 2014.

This work was supported by the Science and Engineering Research Board (SERB), Department of Science and Technology, Government of India [grant number SR-S3-MERC-0115-2012].

## References

1. S. Seguy, F.J. Campa, L.N. Lopez de Lacalle, L. Arnaud, G. Desein, G. Aramendi, Toolpath dependent stability lobes for the milling of thin-walled parts. *Int. J. Mach. Mach. Mater.* **4**(4), 377–392 (2008)
2. B. Jabbaripour, M.H. Sadeghi, S. Faridvand, A study of the effects of cutter path strategies and cutting speed variations in milling of thin-walled parts. *The 7th Jordanian International Mechanical Engineering Conference* (2010)
3. R. Izamshah, M.Y. Yuhazri, M. Hadzley, M. Amran, S. Subramonian, Effects of end mill helix angle on accuracy for machining thin-rib aerospace component. *Appl. Mech. Mater.* **315**, 773–777 (2013)
4. X. Jiang, B. Li, J. Yang, X.Y. Zuo, Effects of tool diameters on the residual stress and distortion induced by milling of thin-walled part. *Int. J. Adv. Manuf. Technol.* **68**, 175–186 (2013)
5. I. Tanase, A. Ghionea, I. Ghionea, Measurement and analysis of cutting forces and deformation at milling thin parts. *Proc. Manuf. Syst.* **5**(4), 243–248 (2010)
6. Y. Cao, Y. Bai, Y. He, Y. Li, NC milling deformation analysis of aluminum alloy thin-wall components based on orthogonal cutting experiments on a vertical machining center. *International Conference on Industrial Mechatronics and Automation*, vol. 2, (2010), pp. 91–94
7. S. Seguy, G. Desein, L. Arnaud, Surface roughness variation of thin-wall milling related to modal interactions. *Int. J. Mach. Tools Manuf.* **48**, 261–274 (2008)
8. F.J. Campa, S. Seguy, L.N. Lopez de Lacalle, L. Arnaud, G. Desein, G. Aramendi, Stable milling of thin-walled parts with variable dynamics. *Sixth International Conference on High Speed Machining* (2007)
9. W. Chen, J. Xue, D. Tang, H. Chen, S. Qu, Deformation prediction and error compensation in multilayer milling processes for thin-wall parts. *Int. J. Mach. Tools Manuf.* **49**, 859–864 (2009)
10. S. Ratchev, W. Huang, S. Liu, A.A. Becker, Modeling and simulation environment for machining of low-rigidity components. *J. Mater. Process. Technol.* **153–154**, 67–73 (2004)
11. H. Ning, W. Zhigang, J. Chengyu, Z. Bing, Finite element method analysis and control stratagem for machining deformation of thin-wall components. *J. Mater. Process. Technol.* **139**, 332–336 (2003)
12. J.K. Rai, P. Xirouchakis, Finite element method based machining simulation environment for analyzing part errors induced during milling of thin-wall components. *Int. J. Mach. Tools Manuf.* **48**, 629–643 (2008)
13. S. Ratchev, E. Govender, S. Nikov, K. Phuah, G. Tsiklos, Force and deflection modeling in milling of low-rigidity complex parts. *J. Mater. Process. Technol.* **143–144**, 796–801 (2003)
14. S. Ratchev, S. Nikov, I. Moualek, Material removal simulation of peripheral milling of thin-wall low-rigidity structures using FEA. *Adv. Eng. Softw.* **35**(8–9), 481–491 (2004)
15. T. Aijun, L. Zhanqiang, Deformations of thin-walled plate due to static end milling force. *J. Mater. Process. Technol.* **206**, 345–351 (2008)
16. E. Budak, Mechanics and dynamics of milling thin-walled structures, Ph.D. Thesis, University of British Columbia, 1994
17. T. Sekiguchi, Y. Kagiya and Y. Goshima, Cemented carbide end mill, U.S. Patent 6719501, 2004
18. G.R. Johnson, W.H. Cook, A constitutive model and data for metals subjected to large strains, high strain rates, and high temperatures, in *Proceedings of the 7th International Symposium on Ballistics*, pp. 541–47, 1983
19. J. Liu, Y. Bai, C. Xu, Evaluation of ductile fracture models in finite element simulation of metal cutting processes. *ASME J. Manuf. Sci. Eng.* **136**(1), 011010-1–011010-14 (2013). doi: [10.1115/1.4025625](https://doi.org/10.1115/1.4025625)
20. G.R. Johnson, W.H. Cook, Fracture characteristics of three metals subjected to various strain, strain rates, temperature, and pressures. *J. Eng. Fract. Mech.* **21**, 31–48 (1985)
21. H.B. Wu, S.J. Zhang, 3D FEM simulation of milling process for titanium alloy Ti6Al4V. *Int. J. Adv. Manuf. Tech.* **71**, 1319–1326 (2014)
22. N. Mangalekar, Experimental studies on thin-wall machining of aluminum 8011 alloy, M.Tech. Thesis, Indian Institute of Technology Guwahati, India, 2012
23. A.F. Liu, *Mechanics and mechanisms of fracture: an introduction* (ASM International, Materials Park, OH, 2005), p. 91